Time-Domain Vernier Effect for Ultra-Fast and Ambiguity-Free Optical Transfer Delay Measurement

Lihan Wang, Yue Yang, Qianwen Sang, Jingxian Wang, Xiangchuan Wang, and Shilong Pan, *Fellow, IEEE, Fellow, Optica*

***Abstract*—Optical transfer delay (OTD) measurement is vital in many applications, such as time-frequency transmission, fiber-based distributed coherent systems, and optical sensing systems, where high accuracy and fast speed are the key parameters for OTD measurement. However, existing high-accuracy OTD measurement methods have to make a trade-off between the measurement range and the speed. In this paper, an ambiguity-free OTD measurement method based on the time-domain Vernier (TDV) effect is proposed to enhance the measurement speed. Two pulse trains with different repetition cycles are multiplexed in the time domain. When the measurement time is restricted, two pulse trains will obtain folded OTDs. Based on the TDV effect, the ambiguity-free OTD can be calculated by solving an indefinite equation composed of the folded OTDs. In verification experiments, the refresh rate is improved to 200 kHz when the OTD measurement range is extended to 100 μs. Additionally, a 2.5 GHz carrier signal is modulated in the pulse to further enhance accuracy. By extracting the phase shift of the carrier signal, an accuracy of $\pm$0.5 ps is achieved.**

***Index Terms*—Optical transfer delay measurement, pulse modulation, Vernier effect.**

I. Introduction

FAST and accurate measurement and control of optical transfer delay (OTD) play a pivotal role in various domains, including optical communications [1], [2], quantum networks [3], optical neural networks [4], and optical sensing systems [5], [6]. For example, in the phase-array antenna [7], [8], compromised OTD accuracy would lead to the degradation of beamforming. In a distributed global navigation satellite system, achieving real-time compensation with sub-picosecond accuracy for OTD compensation can improve the baseline accuracy in the vertical direction 2-3 times [9]. Furthermore, distributed coherent aperture radar systems require stringent phase synchronization to achieve coherent synthesis of echoes [10], [11], [12]. This requires the elimination of OTD fluctuations during signal transmission across the various distributed sites. In the bistatic distributed radar, a loss of 0.5 dB in gain is associated with a phase error of 18 deg [12], equivalent to an OTD deviation of 5 ps in the X band. Additionally, mobile sites could construct free-space laser links for signal transmission [13], [14]. It is imperative for the system to rapidly adjust the OTD before the sites exceed the coherence length [12], which requires both high accuracy and speed in measurement. For relative velocities of the order of meters per second, ensuring synchronization accuracy at the picosecond level requires measurement speeds in the tens of kilohertz range.

The OTD to be measured can typically be demodulated in the time domain [15], [16], the frequency domain [17], [18], or the phase domain [19], [20]. In the time domain, OTD is measured directly by calculating the time interval between the probe and the reference signals. Time-domain methods require the use of a broadband receiver, which leads to a lower signal-to-noise ratio (SNR). Using a 10-Gbit/s pseudorandom bit sequence to modulate the probe pulse, the measurement accuracy of the time domain method can achieve $\pm$3.9 ps [16]. However, these methods usually operate offline due to complex signal processes such as averaging, correlation, and filtering. In the frequency domain, optical frequency-modulated continuous-wave (FMCW) provides a fast way for OTD measurement because the dechirp pulse compression can be realized in the analog domain. In [17], researchers employ a pair of complementary FMCW signals to compensate for phase noise, achieving a speed of 33.3 kHz and a range of 5 μs. In the phase domain, the OTD is derived from the phase shift between the probe signal and the local signal. Phase-based methods offer higher accuracy because they allow for the extraction of the phase shift of the signal using a narrow receiver. However, the unambiguous range is restricted to the wavelength of the single-frequency signal, necessitating a phase unwrapping process to broaden the measurement range. Li et al. [19] proposed a phase-derived ranging method based on microwave frequency sweeping. To reduce the number of frequency points required for the absolute measurement of OTD, they proposed a nonlinear frequency sweep method with a refresh rate of 20.8 Hz [20]. The primary limitation of these methods lies in the switching time of the microwave signal.

The above methods based on single-domain measurement generally have limited performance and difficulty in achieving high accuracy, speed, and range simultaneously. Various multi-domain measurement methods have been recently proposed for enhancing the measurement performance. These methods focus on optimizing the design and characteristics of the probe signal,

Received 9 April 2024; revised 7 January 2025; accepted 9 February 2025. Date of publication 11 February 2025; date of current version 16 May 2025. This work was supported by the National Natural Science Foundation of China under Grant 62075095 and Grant 62271249, and in part by the Funding for Outstanding Doctoral Dissertation in NUAA under Grant BCXJ24-09. *(Corresponding author: Xiangchuan Wang.)*

The authors are with the National Key Laboratory of Microwave Photonics, Nanjing University of Aeronautics and Astronautics, Nanjing 210016, China (e-mail: andwwlh@nuaa.edu.cn; wangxch@nuaa.edu.cn).

Color versions of one or more figures in this article are available at https://doi.org/10.1109/JLT.2025.3541121.

Digital Object Identifier 10.1109/JLT.2025.3541121

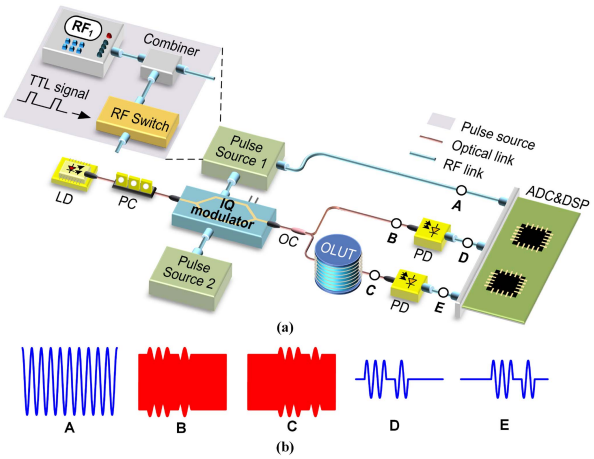

Fig. 1. (a) Schematic configuration of the TDV-based OTD measurement system. (b) Waveform of the signal. LD, laser diode. PC, polarization controller. IQ, in-phase and quadrature. RF, radio-frequency. TTL, transistor-transistor logic signal. OC, optical coupler. OLUT, optical link under test. PD, photodetector. ADC, analog-to-digital converter. DSP, digital signal processor.

utilizing both high-accuracy phase detection and rapid phase unwrapping. In [21], an optical frequency comb with a nonlinear frequency interval is generated for OTD measurement. Although it allows for the parallel extraction of the phase change of each frequency component, this method requires a long accumulation time to separate the frequency components. Other methods, including time-multiplexed [22] and frequency-multiplexed [23] approaches, bypass the microwave frequency sweeping process in phase-derived ranging by using resources from other domains. However, the measurement speed of these methods remains limited to the order of kHz.

This article demonstrates a novel measurement system based on the time-domain Vernier (TDV) effect that offers both a wide range and high speed. The TDV effect is realized by multiplexing two pulse trains with different repetition frequencies in the time domain. Each pulse train generates a folded OTD measurement result when the measurement time is restricted. The ambiguity-free OTD is then resolved by solving the indefinite equation composed of the folded OTDs. To further enhance accuracy, the carrier phase of the pulse train is extracted for OTD measurement. Due to multiplexing the two pulse trains in the time domain, the measurable range is extended to a hundred times compared to the traditional method. In the experiments, the TDV-based measurement system realizes a measurement range of 100 μs, an accuracy of $\pm$0.5 ps, and a refresh rate of 200 kHz.

II. Principle

A. System Configuration

Fig. 1(a) shows the schematic configuration of the TDV-based OTD measurement system. In this system, a laser diode (LD) generates a single-frequency continuous-wave light. The light is then introduced into an in-phase and quadrature (IQ) modulator. To achieve the TDV effect, it is necessary to generate two pulse trains with different repetition cycles. For this purpose, the modulation signal in the IQ modulator is produced using two pulse sources. These sources consist of a radio-frequency (RF) source, which is modulated by an RF switch. The specific mathematical formulation of these required pulse trains is as follows:

$$s(t)=\sum_{m=1}^{2}\sum_{k=-\infty}^{+\infty}\mathrm{rect}\left(\frac{t-kT_{\mathrm{pr},m}}{T_{\mathrm{pw},m}}\right)\cdot\cos(2\pi f(t-kT_{\mathrm{pr},m})), \tag{1}$$

where k is the index number of the pulse train, $T_{\mathrm{pr},m}$ and $T_{\mathrm{pw},m}$ are the repetition cycle and pulse width of the m^{th} pulse train, respectively, f is the frequency of RF, and rect(t) is the rectangular function to describe the shape of the pulse. This function is defined in such a way that $\mathrm{rect}(|t|\leq 0.5)=1$ and $\mathrm{rect}(|t|\geq 0.5)=1$. The output signal of MZM, which is biased at the quadrature point, can be expressed as follows:

$$E_o(t)=E_o(1+M\cdot s(t))\exp(-j2\pi f_c t), \tag{2}$$

where E_o is the amplitude of the optical signal, f_c is the optical carrier frequency, M is the modulation index. With small signal modulation, $M<<1$ is expected. In fact, a dual-driven Mach-Zehnder modulator (DDMZM) can also achieve this function. The DDMZM has a lower optical power insertion loss but exhibits poorer modulation linearity because it does not operate in a push-pull state, compared to an IQ modulator.

After the electro-optical modulation, the modulated optical signal is divided into two parts by a 50:50 optical coupler (OC). The optical signal in the upper branch is considered the reference pulse signal, while the signal in the lower branch is the probe signal. The probe signal is transmitted through the optical link under test (OLUT). The probe and reference signal are detected by two photodetectors (PDs). Considering $M<<1$, the second and higher harmonics in the photocurrent can be ignored. Finally, we can obtain the probe photocurrent $i_{\mathrm{pb}}(t)$ and the reference photocurrent $i_{\mathrm{ref}}(t)$ in an analog-to-digital converter (ADC):

$$i_{\mathrm{pb}}(t)=\eta\alpha^2E_o^2M\cdot s(t-\tau_{\mathrm{pb}}), \tag{3}$$

$$i_{\mathrm{ref}}(t)=\eta E_o^2M\cdot s(t-\tau_{\mathrm{ref}}), \tag{4}$$

where η is the responsivity of the photodetector, α is the transmission loss of the OLUT, τ_{pb} and τ_{ref} represent the OLUT of the probe link and the reference link, respectively.

Assuming the OLUT is a linear transmission system, the RF signal is also sampled by the ADC for phase detection:

$$s_{\mathrm{RF}}(t)=E_s\cdot\cos(2\pi ft). \tag{5}$$

From (3)$\sim$(5), the measured OTD $\tau=\tau_{\mathrm{pb}}-\tau_{\mathrm{ref}}$ is mapped to the time difference between the pulse trains. In addition, the OTD τ is converted into the phase difference in the RF signal, which can be written as $2\pi f\tau$. However, the accuracy of the time difference between the two pulses is influenced by the pulse width and sampling rate. The detected phase difference φ between the two photocurrents has a limited range from $-\pi$ to π, that is,

$$\varphi=-2\pi\left(f\tau-\left\lfloor f\tau+\frac{1}{2}\right\rfloor\right)\pm\delta\varphi, \tag{6}$$

where $\delta\varphi$ is the error that originates from the phase detector, and $\lfloor\ldots\rfloor$ is the floor function.

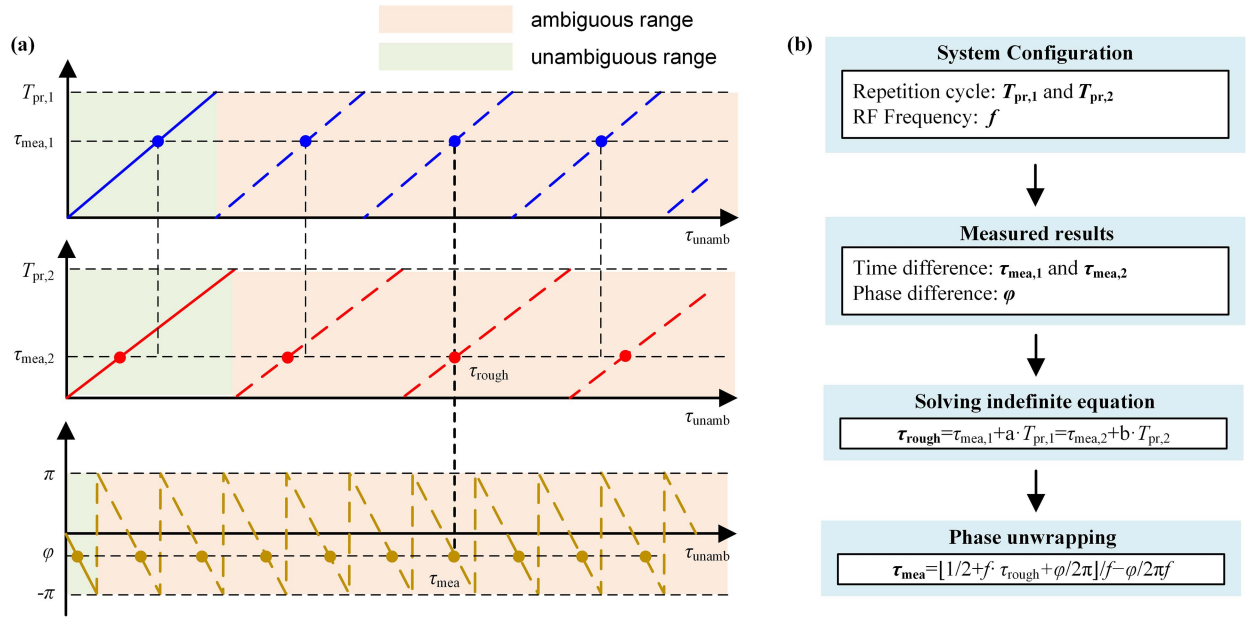

Fig. 2. (a) Principle and (b) Flow chart of the TDV-based OTD measurement method. $T_{\mathrm{pr},m}$ is the repetition cycle of the m^{th} pulse train. $\tau_{\mathrm{mea},m}$ is the measured OTD by applying the m^{th} pulse train. φ is the phase difference between the RF and the probe signal. τ_{unamb} is the absolute OTD without ambiguity. τ_{rough} is the resolved OTD based on TDV. τ_{mea} is the measured OTD based on TDV and phase unwrapping.

The proposed measurement method is based on an incoherent optical system, which experiences negligible optical phase noise and polarization drift compared to coherent measurement systems [24]. Consequently, it can achieve large-range measurements with relatively low system complexity.

In the next part, we will illustrate the principle of the TDV effect to realize high speed and unambiguous range measurement in a limited acquisition duration.

B. TDV-Based OTD Measurement

Fig. 2(a) shows the principle of the TDV-based OTD measurement method. The first step is to solve the ambiguity of the OTD using the Vernier effect. The time difference between the probe and reference photocurrent can be directly extracted using the cross-correlation algorithm. However, the measured time delay range is limited by the pulse repetition cycle, which can be written as $\tau_{\mathrm{mea},m}$:

$$\tau_{\mathrm{mea},m} = \tau \pm \delta\tau - \left\lfloor \frac{\tau}{T_{\mathrm{pr},m}} \right\rfloor \cdot T_{\mathrm{pr},m}, \tag{7}$$

where $\delta\tau$ represents the measurement error induced by ADC and time difference extraction algorithm, and $\lfloor \ldots \rfloor$ is the floor function used to ensure that the $\tau_{\mathrm{mea},m}$ is confined within the range of the $T_{\mathrm{pr},m}$. To obtain the unambiguous OTD, the integer ambiguity $\lfloor \tau/T_{\mathrm{pr},m} \rfloor$ should be resolved. An indefinite equation is constructed as:

$$\tau_{\mathrm{rough}} = \tau_{\mathrm{mea},1} + a \cdot T_{\mathrm{pr},1} = \tau_{\mathrm{mea},2} + b \cdot T_{\mathrm{pr},2}, \tag{8}$$

where τ_{rough} is the resolved OTD measured based on the Vernier effect. If $2|\delta\tau| < |T_{\mathrm{pr},1} - T_{\mathrm{pr},2}|$ and $0.5 < T_{\mathrm{pr},1}/T_{\mathrm{pr},2} < 2$ are valid, the minimum positive integer pair $\{a, b\}$ is the solution of $\{\lfloor \tau/T_{\mathrm{pr},1} \rfloor, \lfloor \tau/T_{\mathrm{pr},2} \rfloor\}$. By utilizing the Vernier effect, the measurement range is broadened from $\mathrm{MAX}\{T_{\mathrm{pr},1}, T_{\mathrm{pr},2}\}$ to $\mathrm{LCM}\{T_{\mathrm{pr},1}, T_{\mathrm{pr},2}\}$, where $\mathrm{LCM}\{\ldots\}$ is the least common multiply operator. When the unambiguous OTD is obtained, a phase unwrapping process can be performed:

$$\tau_{\mathrm{mea}} = \frac{1}{f}\left\lfloor \frac{1}{2} + f\tau_{\mathrm{rough}} + \frac{\varphi}{2\pi} \right\rfloor - \frac{\varphi}{2\pi f}. \tag{9}$$

In order to validate the effectiveness of the proposed phase unwrapping method, we can substitute (6) and $\tau_{\mathrm{rough}} = \tau \pm \delta\tau$ into (9):

$$\tau_{\mathrm{mea}} = \tau \pm \frac{\varphi}{2\pi f} - \frac{1}{f}\left(\left\lfloor f\tau + \frac{1}{2} \right\rfloor - \left\lfloor \left\lfloor f\tau + \frac{1}{2} \right\rfloor + \frac{1}{2} \pm f\delta\tau \pm \frac{\delta\varphi}{2\pi} \right\rfloor \right). \tag{10}$$

From (10), the measured OTD achieves both a broad unambiguous range and high accuracy. For digital signals after sampling, the minimum time interval is the reciprocal of the sampling rate, typically ranging from hundreds of picoseconds to nanoseconds. By performing phase detection on a carrier signal, it is possible to overcome the limitations of the sampling rate and enhance the accuracy of delay measurements to the picosecond or even sub-picosecond level [19].

In addition, $\tau_{\mathrm{mea}} = \tau \pm \delta\varphi/2\pi f$ is established if and only if the time difference error $\delta\tau$ satisfies:

$$\left| f\delta\tau + \frac{\delta\varphi}{2\pi} \right| \leq \frac{1}{2}. \tag{11}$$

Above all, the whole flow chart of the TDV-based OTD measurement method is given in Fig. 2(b).

III. Experiments and Discussions

An experiment was performed based on the configuration shown in Fig. 1(a) to investigate the feasibility and performance of the proposed TDV-based OTD measurement method. A continuous wave laser source (Teraxion PS-NLL) generated the optical signal, which was modulated by an IQ modulator (Fujistu FTM7961). The driven signal, i.e., two electrical pulse trains, of the IQ modulator was generated by an arbitrary waveform generator (AWG, Keysight M8195 A). Two pulse trains shared the same pulse width of 10 ns. The frequencies of the RF signals in the pulse train were 2.5 GHz and 3 GHz, respectively. The repetition cycles of the two pulse trains were 1 μs and 1.012 μs. The AWG also generated a continuous RF signal, which had the same frequency and phase as the carrier of the first pulse. Two 20 GHz PDs (Picometrix P-18A) were applied to convert the optical signals into photocurrents. A 4-port oscilloscope (Agilent DSO9404A) with a sampling rate of 10 GSa/s served as an ADC. Thus, the time deviation was calculated to be less than (1 Sa)/(10 GSa/s) $=$ 0.1 ns. The phase detection process was executed using the fast Fourier transform (FFT) algorithm in the digital domain. The time difference between the pulse trains was extracted by calculating the cross-correlation between the probe and the reference photocurrent.

A. System Accuracy and Stability

In the proposed TDV-based OTD measurement system, the time duration of phase detection is limited to one pulse width. To determine the choice of pulse width, we tested the relationship between the measured phase variance and the window size in FFT. The frequency of the RF signal, designated for phase detection, is set at 2.5 GHz. According to (11), the phase error is required to be less than 0.5π . Fig. 3(a) shows the results obtained from a measurement repeated 500 times. By using a larger window size in the FFT, more data points are included in the phase detection, allowing for a better estimation of the phase and reducing the impact of quantization noise and white noise. However, a large pulse width could lead to the overlap of the two pulse sequences in the time domain, resulting in the invalidation of the TDV-based time difference extraction. When the window size of FFT is 10 ns, the phase variance is 0.079 deg^2.

In the proposed system, the measurement error of the OTD is solely determined by phase detection when (11) is effective. To assess the stability and accuracy of the system, the performance of the phase detection is verified. The fluctuation of the system over a period of 1000 seconds, depicted in Fig. 3(b), follows a normal distribution. The standard deviation of the OTD fluctuation is measured at 0.299 ps, which is equivalent to 0.0724 deg^2 in phase variance ($\sigma_\varphi^2 = 4\pi^2 f^2 \sigma_\tau^2$). This value is aligned with the value of 0.079 deg^2 in Fig. 3(a). In addition, an electrically controlled optical delay line (ODL, General Photonics MDL-002) is inserted into the OLUT. Fig. 3(c) and (d) show the measured delay and deviation when the ODL sweeps from 0 ps to 20 ps at 2 ps intervals, showing that the measured error is less than $\pm$0.5 ps.

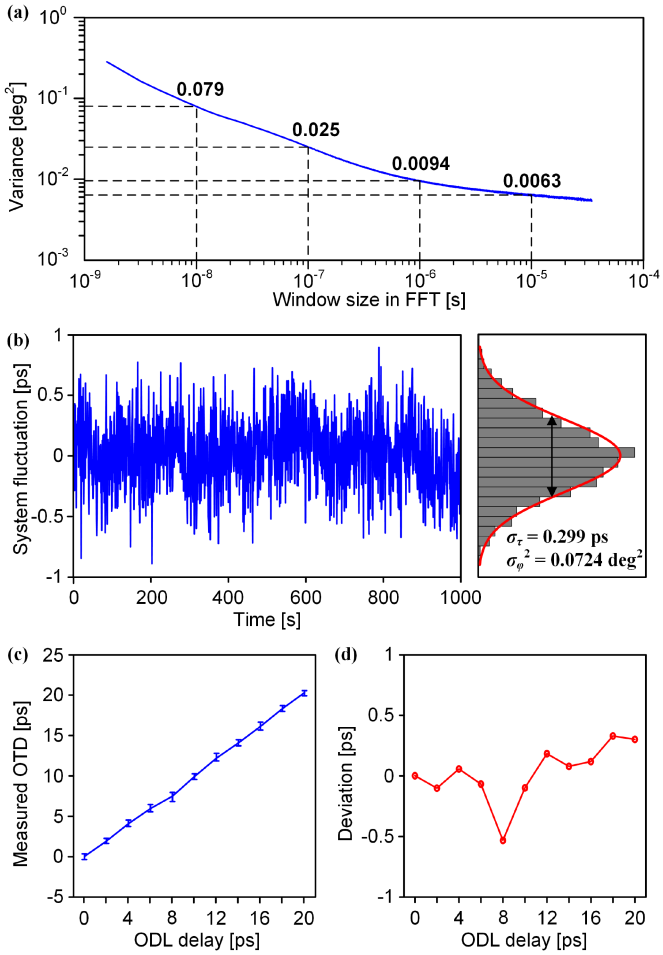

Fig. 3. (a) Measured phase variance corresponds to the window size in FFT. (b) The fluctuation and histogram of the system over a period of 1000 seconds. (c) Measured OTD and (d) the deviation when the optical delay line sweeps from 0 ps to 20 ps at intervals of 2 ps.

B. High Accuracy OTD Measurement Based on Phase Unwrapping

To access the effectiveness of phase unwrapping, an electrically controlled ODL and an optical fiber of a fixed 3.5-meter length were employed as the OLUT in the experiments. Fig. 4(a) shows the time-domain waveform of photocurrents and RF signal collected from the 4-port oscilloscope, the photocurrents in Fig. 4(a) contain only the first pulse train. Since the measured OTD is within the range of pulse repetition periods $T_{\mathrm{pr},1}$ and $T_{\mathrm{pr},2}$, the solution for the pair of integers $\{\lfloor \tau/T_{\mathrm{pr},1} \rfloor, \lfloor \tau/T_{\mathrm{pr},2} \rfloor\}$, which represents the index number of the pulse train, is $\{0, 0\}$. This indicates that complete pulse periods of $T_{\mathrm{pr},1}$ or $T_{\mathrm{pr},2}$ are not within the measured OTD duration. In this case, to obtain an unambiguous OTD, we should only extract the phase difference between the photocurrents and the time difference between the two pulses.

By comparing the phase differences between the photocurrents and the RF signal, the phase difference can be extracted, which are $\Delta\varphi_1 = 0.3892$ rad and $\Delta\varphi_2 = -1.715$ rad. The phase difference between i_{pb} and i_{ref} can be obtained by

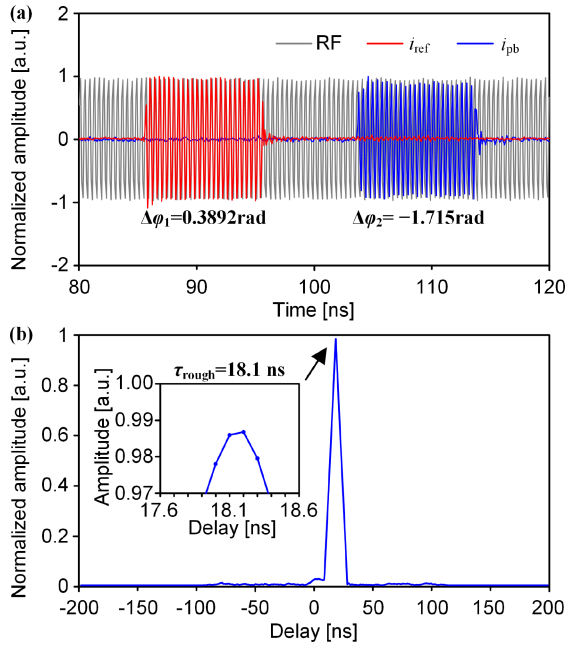

Fig. 4. (a) Time-domain waveform of the photocurrents and RF. $\Delta\varphi_1$ is the detected phase difference between probe photocurrent and RF; $\Delta\varphi_2$ is the detected phase difference between reference photocurrent and RF. (b) Normalized cross-correlation between the probe and reference photocurrent.

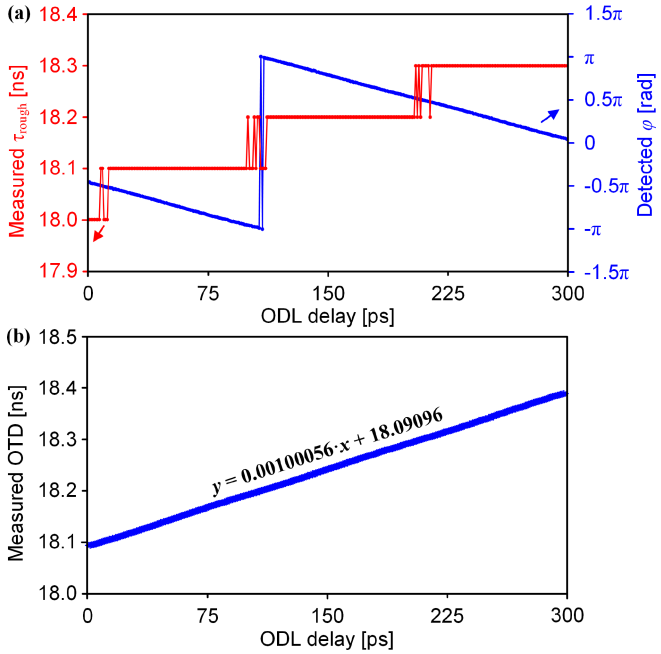

Fig. 5. (a) Measured time difference τ_{rough}, detected phase difference φ, and (b) measured OTD when the ODL is swept from 0 ps to 300 ps at intervals of 1 ps.

calculating $\varphi = \Delta\varphi_2 - \Delta\varphi_1 = -1.715\ \text{rad} - 0.3892\ \text{rad} = -2.1042\ \text{rad}$.

According to (11), if we neglect the phase error, the time difference error should be less than $1/2f = 0.2$ ns . Here, the time difference between the two pulses is calculated using the cross-correlation algorithm, which is shown in Fig. 4(b). As can be seen, the maximum value of cross-correlation is between 18.1 and 18.2 ns. Therefore, the value of τ_{rough} can be regarded as 18.1 ns. Substituting these results into (9), the measured OTD can be obtained by $\tau = (\lfloor 18.1\ \text{ns} \times 2.5\ \text{GHz} + 0.5 - 2.1042/2\pi \rfloor + 2.1042/2\pi)/2.5\ \text{GHz} = 18.13396\ \text{ns}$.

To validate the effectiveness of the phase unwrapping algorithm, the ODL is swept from 0 ps to 300 ps at intervals of 1 ps. The measured time difference τ_{rough} and the detected phase difference φ are shown in Fig. 5(a). Since the sampling rate is 10 GHz, the minimum measurable time difference is 0.1 ns (1/10 GHz). The variable delay line with a range of 300 ps would introduce three jumps in time difference. The modulation frequency is 2.5 GHz, which means that the phase difference φ would be phase shifted by 1.5π rad ($2\pi \times 300$ ps $\times$ 2.5 GHz). Fig. 5(b) shows the result of the OTD calculation using (9). The figure demonstrates high linearity with a slope of 1.00056 ps/ps and an R-square value of 0.999923. These results indicate that the phase unwrapping method is valid for each OTD over a change range of 300 ps.

The proposed method obtains the pulse time difference through a cross-correlation algorithm. It should be noted that the cross-correlation operation can also be performed in the frequency domain by calculating the cross-power spectrum. Therefore, the actual demodulation process can be carried out by performing FFT operations on the sampled signals for convenience. This is followed by frequency domain cross-correlation and phase detection, which directly obtain the measured delay.

C. Large OTD Measurement Based on Time-Domain Vernier Effect

In the proposed method, the two pulse trains are generated simultaneously. Which means that the specific index pulses would overlap. The overlapped pulses result in interference for time difference measurement, as illustrated in Fig. 6(a). In the system, the total period of the pulse train is the least common multiple between the two pulse repetition cycles, that is, $\mathrm{LCM}(1\ \mu\text{s}, 1.012\ \mu\text{s}) = 253\ \mu\text{s}$. Fig. 6(b) shows the time-domain waveform of the two photocurrents when the OLUT is a 10-km optical fiber. In the whole period of the pulse train, the two pulse trains would overlap 5 times. For the pulse train with a repetition cycle of $1.012\ \mu$s, the overlapped pulse indexes are 1, 83, 84, 166, and 167. To avoid the pulse overlapping, the sampling time length of the TDV-based method is set as $5\ \mu$s, which contains at least four pulses.

We performed individual measurements on optical fibers with lengths of 20 km, 10 km, and 8 km. The corresponding time-domain waveforms are depicted in Fig. 7(a) to (c), where the two pulse trains are labeled s_1 and s_2. These pulse trains can be easily distinguished in the time-domain waveform owing to their different frequencies. The cross-correlation results between the two photocurrents are presented in Fig. 7(d) to (f). The four peaks in the cross-correlation result indicate the delay differences among the various pulses. The rough delay of the pulse train can be extracted from the cross-correlation due to the presence of a specific lead-lag

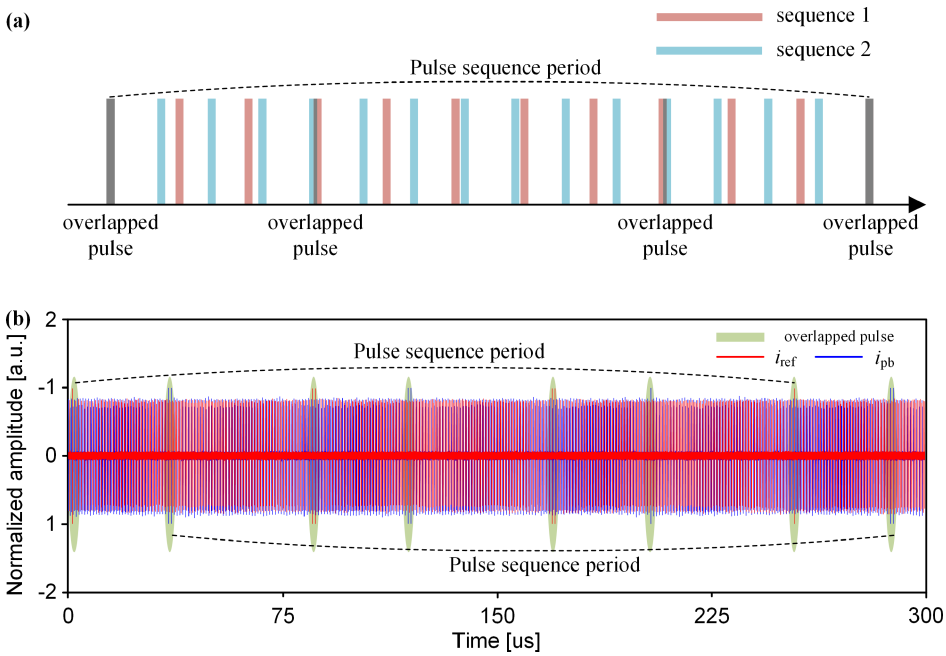

Fig. 6. (a) Illustration of the time-domain waveform of the photocurrents. (b) Time-domain waveform of the photocurrents within 300 μs when the OLUT is a 10-km optical fiber. The green rectangle represents the overlapped portion of the pulse trains. The blue line is the probe photocurrent and red line is the reference photocurrent. The period of the pulse train is 253 μs.

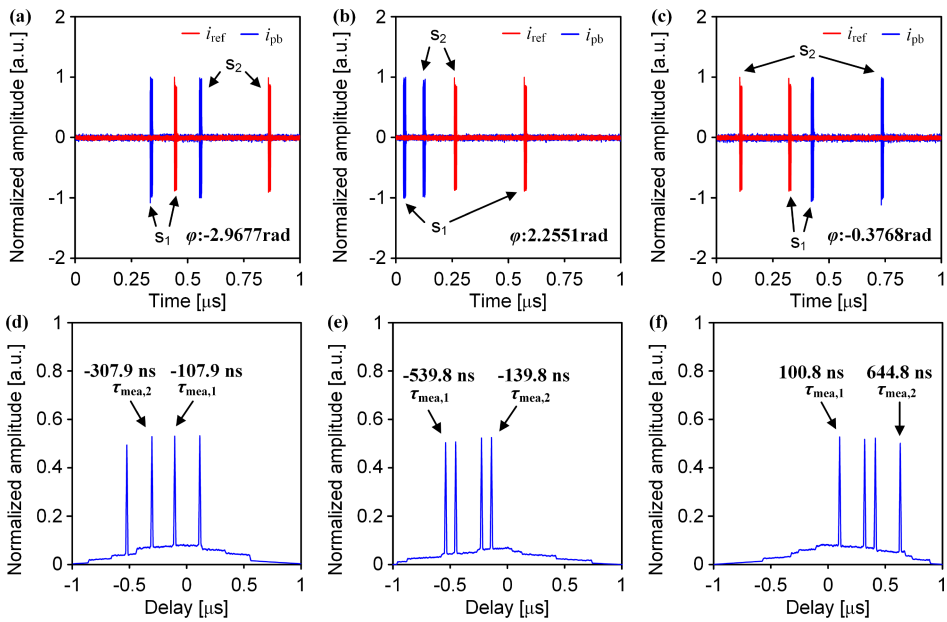

Fig. 7. (a)∼(c) Time-domain waveforms of the probe and reference photocurrent within a 1 μs interval when using optical fibers of 20 km, 10 km, and 8 km lengths as the DUT. s_1 and s_2 belong to two different pulse trains. (d)∼ (f) Normalized cross-correlation between the probe and reference photocurrent when using optical fibers of 20 km, 10 km, and 8 km lengths as the DUT.

relationship in the time domain. For example, in Fig. 7(d), the measured values of $\tau_{\mathrm{mea},1}$ and $\tau_{\mathrm{mea},2}$ are -107.9 ns and -307.9 ns, respectively. Then, we can form an indefinite equation: $\tau_{\mathrm{rough}} = -0.1079 + 1 \times a = -0.3079 + 1.012 \times b$. Upon solving this, the minimum integer pair for $\{a, b\}$ is calculated to be $\{101, 100\}$, resulting in a value τ_{rough} of $100.8921\,\mu$s. The measured OTD can be calculated as $\tau = (\lfloor 100.8921\,\mu\mathrm{s} \times 2.5 \quad \mathrm{GHz} + 0.5 - 2.9677/2\pi \rfloor + 2.9677/2\pi)/2.5 \quad \mathrm{GHz} = 100.89218893\,\mu$s. Similarly, for Fig. 7(e) and (f), the integer pairs for $\{a, b\}$ are determined to be $\{51, 50\}$ and $\{39, 38\}$, resulting in final measured OTDs of $50.46025644\,\mu$s and $39.10082599\,\mu$s, respectively.

TABLE I
COMPARISION OF FAST OTD MEASUREMENT METHODS [16], [17], [20], [21], [22], [23]

Types	Methods	Refresh rate	Range	Accuracy	Signal source	Demodulation
Time domain	Correlation OTDR [16]	sub Hz	500 μs	±3.9 ps	A PRBS generator	Cross-correlation
Frequency domain	Optical FMCW [17]	33 KHz	5 μs	±0.42 ps	An LFM signal source, a single-tone signal source	Hilbert transform
Phase domain	Phase-derived ranging [20]	20.8 Hz	185 μs	±0.04 ps	A VNA	Linear fitting
Multi-domain	Optical frequency comb [21]	1 kHz	1.67 μs	±0.19 ps	Two single-tone sources	FFT, linear fitting
	Time-multiplexed signal [22]	0.83 kHz	75 μs	±0.1 ps	An LFM signal source, a single-tone signal source	FFT
	Frequency-multiplexed signal [23]	1.7 kHz	1.67 μs	±0.29 ps	An LFM signal source, a VNA	FFT
	Proposed TDV-based method	200 kHz	100 μs	±0.5 ps	Two electrical pulse generators, a single-tone signal source	FFT

PRBS: pseudo-random bit sequence.

In real-time implementation, the TDV-based OTD measurement can be achieved without the need for high-speed ADCs or digital signal processors. For instance, the time difference between two pulses can be directly obtained using a commercial FPGA with trigger and counter functionality. Additionally, phase detection can be efficiently performed through down-conversion and IQ demodulation at the baseband.

IV. CONCLUSION

The performance of fast OTD measurement methods is compared in Table I. Among these, methods based on single-domain measurement exhibit limited performance. The time domain method is capable of large-range measurement, but enhancing its accuracy requires extensive time accumulation. Conversely, the frequency domain method is constrained by a limited range due to its unbalanced response within its bandwidth. The phase domain method offers both a large range and high accuracy. However, the frequency sweep process is time-consuming. Methods employing multi-domain measurement address this problem, marking the first demonstration of a refresh rate in the hundred kilohertz and a range in the hundred microsecond domain, while maintaining sub-picosecond accuracy. The ambiguity-free OTD is resolved by solving the indefinite equation composed of the two pulse trains. The carrier phase shift of the pulse train is extracted to improve the OTD accuracy. In verification experiments, the measurement range is extended to 100 μs when the accumulation time is 5 μs . Additionally, a 2.5 GHz carrier signal is modulated in the pulse to further enhance accuracy. By extracting the phase shift of the carrier signal, an accuracy of ± 0.5 ps is achieved. In addition, the performance enhancement offered by the proposed OTD measurement method does not require a significant increase in system complexity. In the system, we replaced the linear frequency modulated (LFM) signal sources or broadband vector network analyzers (VNA) typically required in traditional measurement with two 10-ns level electrical pulse generators. The demodulation process in the proposed method only requires performing a FFT operation, which is compatible with existing typical measurement methods. The proposed TDV-based OTD measurement method enables accurate and reliable OTD measurements, especially valuable in fiber-based networks where high-speed and large-range measurements are essential.

REFERENCES

[1] I. Khader, H. Bergeron, L. C. Sinclair, W. C. Swann, N. R. Newbury, and J.-D. Deschênes, "Time synchronization over a free-space optical communication channel," *Optica*, vol. 5, no. 12, pp. 1542–1548, 2018.

[2] D. Chitimalla, K. Kondepu, L. Valcarenghi, M. Tornatore, and B. Mukherjee, "5G fronthaul–latency and jitter studies of CPRI over ethernet," *J. Opt. Commun. Netw.*, vol. 9, no. 2, pp. 172–182, 2017.

[3] R. Valivarthi et al., "Picosecond synchronization system for quantum networks," *J. Lightw. Technol.*, vol. 40, no. 23, pp. 7668–7675, Dec. 2022.

[4] J. Liu et al., "Research progress in optical neural networks: Theory, applications and developments," *PhotoniX*, vol. 2, pp. 1–39, 2021.

[5] L. Wang, Y. Fang, S. Li, X. Wang, and S. Pan, "FBG demodulation with enhanced performance based on optical fiber relative delay measurement," *IEEE Photon. Technol. Lett.*, vol. 32, no. 13, pp. 775–778, Jul. 2020.

[6] W. Yuan, B. Pang, J. Bo, and X. Qian, "Fiber optic line-based sensor employing time delay estimation for disturbance detection and location," *J. Lightw. Technol.*, vol. 32, no. 5, pp. 1032–1037, Mar. 2014.

[7] I. Frigyes and A. J. Seeds, "Optically generated true-time delay in phased-array antennas," *IEEE Trans. Microw. Theory Tech.*, vol. 43, no. 9, pp. 2378–2386, Sep. 1995.

[8] M. Y. Frankel and R. D. Esman, "True time-delay fiber-optic control of an ultrawideband array transmitter/receiver with multibeam capability," *IEEE Trans. Microw. Theory Tech.*, vol. 43, no. 9, pp. 2387–2394, Sep. 1995.

[9] X. Jiang, X. Wang, A. Zhao, J. Yao, and S. Pan, "A multi-antenna GNSS-over-fiber system for high accuracy three-dimensional baseline measurement," *J. Lightw. Technol.*, vol. 37, no. 17, pp. 4201–4209, Sep. 2019.

[10] X. Xiao et al., "Photonics-based wideband distributed coherent aperture radar system," *Opt. Exp.*, vol. 26, no. 26, pp. 33783–33796, 2018.

[11] X. Xiao, S. Li, S. Peng, X. Xue, X. Zheng, and B. Zhou, "Microwave photonic wideband distributed coherent aperture radar with high robustness to time synchronization error," *J. Lightw. Technol.*, vol. 39, no. 2, pp. 347–356, Jan. 2021.

[12] J. A. Nanzer, S. R. Mghabghab, S. M. Ellison, and A. Schlegel, "Distributed phased arrays: Challenges and recent advances," *IEEE Trans. Microw. Theory Tech.*, vol. 69, no. 11, pp. 4893–4907, Nov. 2021.

[13] D. R. Gozzard, L. A. Howard, B. P. Dix-Matthews, S. Karpathakis, C. Gravestock, and S. W. Schediwy, "Ultrastable free-space laser links for a global network of optical atomic clocks," *Phys. Rev. Lett.*, vol. 128, no. 2, 2022, Art. no. 020801.

[14] A. U. Chaudhry and H. Yanikomeroglu, "Laser intersatellite links in a starlink constellation: A classification and analysis," *IEEE Veh. Technol. Mag.*, vol. 16, no. 2, pp. 48–56, Jun. 2021.

[15] M. Barnoski, M. Rourke, S. Jensen, and R. Melville, "Optical time domain reflectometer," *Appl. Opt.*, vol. 16, no. 9, pp. 2375–2379, 1977.

[16] F. Azendorf, A. Dochhan, and M. H. Eiselt, "Accurate single-ended measurement of propagation delay in fiber using correlation optical time domain reflectometry," *J. Lightw. Technol.*, vol. 39, no. 18, pp. 5744–5752, Sep. 2021.

[17] Y. Zhang et al., "Ultrafast and high-precision time delay measurement based on complementary frequency-swept light and frequency-shifted dechirping," *J. Lightw. Technol.*, vol. 42, no. 6, pp. 1927–1933, Mar. 2024.

[18] K. Yuksel, M. Wuilpart, V. Moeyaert, and P. Mégret, "Optical frequency domain reflectometry: A review," in *Proc. 11th Int. Conf. Transparent Opt. Netw.*, 2009, pp. 1–5.

[19] S. Li et al., "Optical fiber transfer delay measurement based on phase-derived ranging," *IEEE Photon. Technol. Lett.*, vol. 31, no. 16, pp. 1351–1354, Aug. 2019.

[20] S. Li, T. Qing, J. Fu, X. Wang, and S. Pan, "High-accuracy and fast measurement of optical transfer delay," *IEEE Trans. Instrum. Meas.*, vol. 70, 2020, Art. no. 8000204.

[21] X. Liu et al., "Optical transfer delay measurement based on multi-frequency phase-derived ranging," in *Proc. 19th Int. Conf. Opt. Commun. Netw.*, 2021, pp. 1–6.

[22] Q. Sun, C. Liu, J. Yang, J. Liu, J. Dong, and W. Li, "Phase-derived ranging based fiber transfer delay measurement using a composite signal for distributed radars with fiber networks," *Photonics*, vol. 10, no. 4, 2023, Art. no. 421.

[23] B. Qiu et al., "Laser ranging with micrometer precision and kHz rate via joint frequency-phase measurement," *IEEE Photon. Technol. Lett.*, vol. 34, no. 22, pp. 1214–1217, Nov. 2022.

[24] L. Wang, X. Wang, S. Li, and S. Pan, "Coherent optical phase-derived ranging with high sensitivity and accuracy," *J. Lightw. Technol.*, vol. 42, no. 2, pp. 579–581, Jan. 2024.